CHAPTER 1

INTRODUCTION AND LITERATURE REVIEW

1.1 Introduction

The extensive usage of microwave-based devices, such as High-power microwaves (HPM), has been prevalent in the microwave world during the last few decades due to its numerous civilian and military applications, as well as the overall technological breakthrough for device development. The ability to generate RF in millimetre-wave ranges and dual-frequency generation with a single HPM device has piqued the interest of researchers and academics worldwide. The broad category of conventional HPM covers microwave and millimetre-wave frequency ranges (1-300 GHz), peak power is greater than 100 MW, or pulse energy is less than 1KJ. It is also classified as (1) the high PRF (Pulse Repetition Frequency), Pulse of long duration or continuous wave (CW), (2) the low PRF or single-shot sources, pule of short duration, high peak power, and amplifiers.

1.2 Origin and Classification of HPM

Microwave-based devices are categorized into two types, i.e. conventional microwave devices (i.e., Klystron, Magnetron, TWT, BWO, etc.) and High Power microwave devices (i.e., Relativistic Klystron, Relativistic Magnetron, VIRCATOR, Reltron, FEL, MILO, etc.). The first cavity-type microwave device was Klystron, developed in 1937. During the Second World War (1939-1945), very rapid development occurred in microwave technology, which included the development of the magnetron as well as the inventions of the travelling wave tube (TWT) and the backward wave oscillator (BWO). In the 1950s,efforts to manage thermonuclear fusion for energy production facilitated the development of gyrotrons to attain high average power for frequencies above 100 GHz. The cross-field amplifier (CFA) was

developed in the 1960s and the subsequent introduction of pulsed power enabled the produce charged particle beams with current and voltage in the range of 10 KA and 1 MV. The charged particle beam generates intense relativistic (i.e. electron energies comparable to or greater than the 511 keV rest energy of an electron) electron beams (IREB) which leads to producing another class of microwave tubes (i.e. HPM devices) like Relativistic Klystron Amplifier (RKA), Relativistic Klystron Oscillator (RKO), Relativistic Magnetron and Relativistic Backward Wave Oscillator (RBWO). This is followed by the development of other HPM sources (i.e., VIRACATOR, Gyro devices, MILO, etc.) in successive years. The newly admitted class of HPM are plasma-assisted devices like Reltron and Arletron. [Benford et al. (2007)]

Microwave tubes are broadly classified based on O- and M-type electron beam characteristics. The linear beam tubes (O-Type) are those where the dc electric field and the dc magnetic field are parallel. In O-type tubes, the kinetic energy of the electron changes into RF energy like klystron, TWT, Reflex klystron, BWO, etc. The cross-field tubes (M-Type), where the dc electric field and the dc magnetic field are perpendicular. In M-Type, the potential energy of the electron changes into RF energy like magnetron, FWCFA, gyrotron etc.

The classification of microwave tubes based on RF phase velocity is slow-wave and fast-wave tubes. Slow space-charge waves are defined as having RF phase velocities whose velocity is less than that of an electron beam in the propagation direction, like relativistic klystron, relativistic magnetron, relativistic backward wave oscillator (RBWO), Magnetically Insulated Line Oscillator (MILO) etc. Fast space charge waves are defined as waves with RF phase velocities faster than electron beam velocity like Gyrodevices etc.

Another classification of HPM is based on the frequency band i.e. narrowband and ultra-wideband electromagnetic radiation HPM sources. Narrowband HPM sources produce

coherent radiation at the loss of the kinetic energy of a mono-energetic electron beam in pulses spanning from 10's to 100's ns in duration. Ultra-wideband sources do not employ an electron beam but rather a large voltage spike with a very short rise time. Due to coupling, the antenna transmits this large voltage spike over a wide frequency range. Flashbulbs are a good analogy for ultra-wideband.

Based on the interaction mechanism between the relativistic electron beam and the RF structure, HPM sources support three electromagnetic (EM) radiation types: Cherenkov radiation, Bremsstrahlung radiation, and Transition radiation.

Cherenkov radiation	**Bremsstrahlung radiation**	**Transition radiation**
When electrons flow through a medium with a high refractive index ($n = c/v > 1$). The phase velocity of electromagnetic waves ($v_{ph} = c/n$) is smaller than velocity (v) of the electrons.	When electron oscillation occurs in an external magnetic and/or electric field. Electromagnetic radiation has a frequency that matches either the Doppler-shifted oscillation frequency of electrons or its harmonics.	Transition radiation occurs when electrons pass through two distinct media with a different refractive index, such as metallic grids or plates.
• RF output power in terms of several GW. • Frequency range- 1-10 GHz • Pulse Length – 10-100ns • Repetition Rate – Several 100 Hz	• Frequency range- above 100 GHz	• RF output power in terms of 10's of GW. • Pulse Length – 100ns • Frequency range- ~ 1 GHz
RBWO, MILO, TWT, Relativistic Magnetron	FEL (Free electron Lasers), CRM (cyclotron resonance masers), Gyrotron	Relativistic klystron oscillator (RKO), Reltron and Relativistic klystron amplifier (RKA)

Vircators, also known as virtual cathode oscillators, are a special case of Bremsstrahlung radiation that oscillates electrons in an external electromagnetic field [Gold and Nusinovich (1997)]. This device can be considered as an extreme version of intense beam relativistic klystron amplifiers (RKAs), in which space-charge induces voltage depression, enhancing electron velocity modulation and bunching significantly.

1.3 Overview and Evaluation of Distinct HPM Tubes

Due to technical advancements around its many civilian and military uses and device development, High-Power Microwaves (HPMs) have become very prominent in the microwave world during the last few decades. Figure 1.1 depicts the range of HPM devices at various frequencies and power levels.

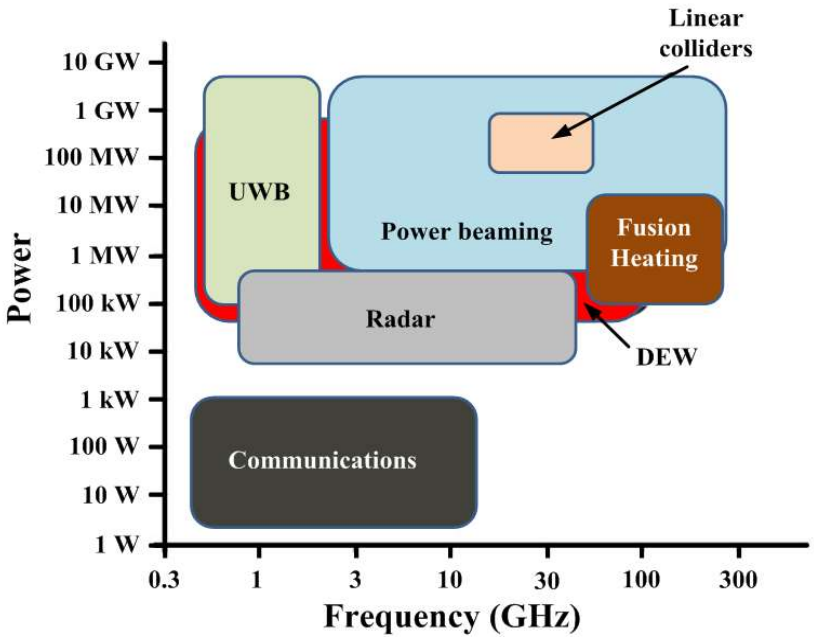

Figure 1.1: HPM application domain at various frequencies and power levels [Benford *et al.* (2007)].

The civilian and military use of HPM is briefly summarised in Table 1.1. HPM devices can be classified as (a) Microwave and millimetre-wave narrow band sources and amplifiers for RF acceleration in high-energy linear colliders. (b) High average power oscillators in resonant heating and current propulsion of thermonuclear fusion plasmas based on prevailing or capable applications of these sources. (c) Wideband millimeter-wave amplifiers for radar and communication systems, and (d) High-peak-power sources for direct energy weaponry (DEW) of both the hard-kill type aimed at physically destroying the targets and the soft-kill type by rendering the enemy's mission-critical components either malfunctioning or defective. To realize this, the peak output power of the RF signal must be in the range of several GW. In contrast, the signal's pulse width should be approximately 100 ns in the microwave and millimetre-wave frequency.

Table 1.1: HPM device application in several domains [Benford *et al.* (2007)].

Military	High Power Microwave (HPM) Electronic Attack Radar: Guidance, Search, Missile-seeker, Track, Weather, Test Electronic Counter Measures(ECM)
Industrial	Industrial plasmas, mainly for semiconductor manufacture Testing and Instrumentation Materials processing
Scientific	Plasma heating and fusion energy research Charged particle accelerators Spectroscopy Materials Processing Research Radio astronomy Ground Penetrating Radar Medical/Biomedical Atmospheric radar
Civilian Infrastructure and consumer markets	Global Positioning System (GPS) Satellite communications

Figure 1.2 shows the block diagram of HPM system. The various blocks of the HPM system play a distinct functions in the RF generation and application process.

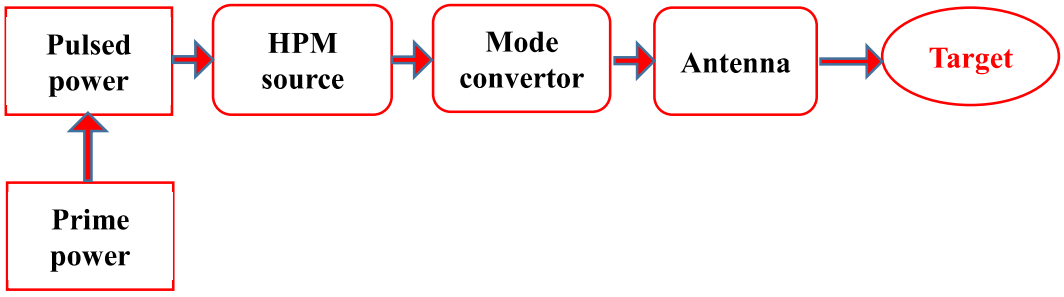

Figure 1.2: Block diagram of an HPM system [Benford *et al.* (2007)].

Prime Power: Prime power supply produces a relatively low-power electrical signal in a long pulse or continuous mode. For attaching the prime power to the pulse power supply, the average power, the repetition rate, which simultaneously sets the energy per pulse, and the output voltage are all crucial factors. Internal combustion is a primary power source which gives AC as the output; an interface constituent such as a pump, motor, controller, or AC to DC converter; and finally, energy storage and electrical source components coupled to an AC or DC converter make up the prime power supply. The pulsed power source receives a sequence of switched DC pulses from the prime power output.

Pulsed Power: HPM sources, in general, require drivers to create short, intense electrical pulses of 1 MV or more and up to 1 microsecond. It can be accomplished by using pulse compression or capacitor banks, which help a low-voltage, a slowly-rising signal is converted into a high-voltage, rapidly-rising signal or inductive energy stored by open switches.

HPM Source: The generation of the electron beam, efficient beam-wave interaction, and extraction of the generated RF signal are the three core processes of the HPM source, which is

the main building block of the overall HPM system. The rudimentary process at the back of all vacuum electron beam sources is the resonant interactions that take between the natural oscillation modes of the electron plasma and the eigenmode of cavities and/or waveguides.

Mode Converter: To achieve optimum target impact requires the radiated EM wave to be in the right mode. Some HPM sources generate azimuthally symmetrical modes with null inside the route of propagation, which is transformed to the required modes with the most electricity inside the route of propagation by using an appropriate mode converter. Consequently, the mode converter is thus used for tailoring the spatial distribution of electromagnetic power to optimize the transmission of RF electricity and coupling to an antenna. Some HPM sources generate azimuthally symmetrical modes having a null in the direction of propagation. Such azimuthally symmetrical modes are converted to required modes having maximum power in the direction of propagation by using a suitable mode converter [Yuan *et al.* (2006)].

Antenna: The microwave radiator, like an antenna, acts as the interface between the HPM supply and the relaxation of the space. The RF power popping out from the mode converter is similarly radiated in the direction of the goal through the antenna, which compresses the output spatially right into a tighter and high-depth beam. The rectangle horn antennas are the most sort of antenna employed in HPM sources.

A brief description of various HPM sources, as well as their step-by-step development, is given below.

1.3.1 Relativistic Klystron Amplifier (RKA), and Relativistic Klystron Oscillator:

Klystrons are transition radiation-based devices. The configuration of the structure can work either in an amplifier or in an oscillator. A conventional klystron amplifier's interaction

structure consists of a fixed buncher cavity and one or more moveable catcher cavities. The electron beam travels from one to the other via a variable-length drift tube. The buncher cavity uses velocity modulation to separate a tumultuous electron beam into bunches. The transit angle must not exceed π radians to keep the appropriate RF phase inside the gap length while generating coherent radiation by decelerating electron bunches in the catcher cavity. The relativistic Klystron is a prominent HPM source in charged particle physics and RF Linear Accelerator (LINAC) applications. The annular beam used in relativistic klystron amplifiers (RKAs) can carry more current (usually 5-20 kA) at the same voltage as a solid pencil beam used in conventional klystrons. The RKA was developed at the Naval Research Laboratory (NRL), and it has demonstrated 15 GW power at 1.3 GHz with a 50 ns pulse and 6 GW power in the single-shot mode for up to 100 ns pulse [Friedman *et al.* (1990)]. In RKA operation, the beam space charge plays a significant role, and a single buncher cavity can create a beam bunching with a 1.5 times higher current in the fundamental harmonic than the DC. Electrons reflexing from virtual cathodes within the cavities caused this great degree of modulation [Friedman *et al.* (1984)]. RKA has a few drawbacks, like i) decreased output power and efficiency at higher frequencies and ii) pulse length and repetition rate limitations due to its beam interception system.

To overcome these shortcomings, a triaxial version of RKA was proposed, in which an annular beam propagates between two coaxial conductors [Friedman *et al.* (1993)]. This arrangement permits almost double the current of the original RKA and requires a lower magnetic field for beam confinement. The greater current combined with the bigger volume resulted in a significant increase in operational power. By utilizing a tri-axial extractor and incorporating a feedback mechanism via electromagnetic coupling between the cavities instead of reflecting the beam, the Friedman RKA was changed to a self-oscillating variation known as

the relativistic klystron oscillator (RKO). This device demonstrated 1.5 GW of power [Hendricks *et al.* (1996)]. The relativistic klystrons can be classified into three types based on their operational characteristics: i) high-impedance near-relativistic klystrons, such as the 2.6 m long, 300 kg klystron built by SLAC for DESY (Deutsches Elektronen-Synchrotron) with 535 kV beam voltage, 700 A beam current, and 150 MW output power at 2.998 GHz frequency. The efficiency was 40%, and the solenoidal coil used 15 kW more power to create a 0.21 T magnetic field [Sprehn *et al.* (1994)]. Later, periodic permanent magnet (PPM) focusing was utilized to preserve electricity and reduce the amount of money spent on electromagnets [Sprehn *et al.* (1996)]. ii) High-impedance relativistic klystrons; the 250 MW SL-4 multi-output klystron with 1.3 MV voltage and 520 A RF current [Allen *et al.* (1989)]. iii) Low-impedance klystron; the annular-beam klystron at NRL with 500 kV, 5 kA input, and 1.7 GW output power at frequency 3.5 GHz [Friedman *et al.* (1988)]. Relativistic klystrons are extensively used as high-energy drivers for free-electron lasers, directed energy weapons, colliders, and accelerators. [Benford *et al.* (2007)].

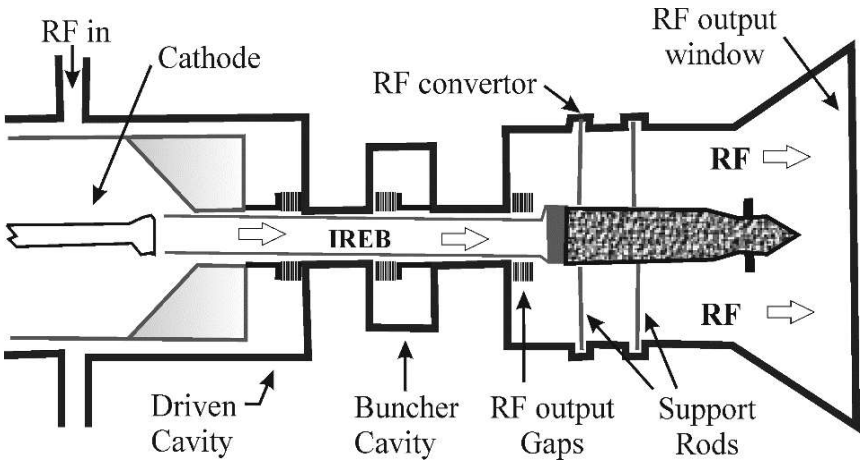

Figure 1.3: Schematic of a Relativistic Klystron Amplifier [Barker and Schamiloglu (2001)].

1.3.2 Relativistic Backward Wave Oscillator (RBWO)

A backward wave oscillator (BWO) is a Cherenkov-type microwave oscillator with a wide frequency coverage range [Barker and Schamiloglu (2001)]. Waves moving in the backward direction with respect to the electron beam are amplified by BWOs. The backward wave first-order spatial harmonic interacts with the beam. A cut-off waveguide reflects the backward wave on the cathode side, and the output is collected at the opposite end. This reflected wave does not interact synchronously with the electron beam. The operating point may be relocated to any position on the area with the negative slope of the dispersion diagram, lying below the light line, by switching the operating voltage and/or the structure period. A Relativistic Backward Wave Oscillator (RBWO) is an HPM device that uses a powerful relativistic electron beam to generate a negative group velocity EM wave, which propagates in the opposite direction of the electron beam. They have undergone significant research activities for more than three decades leading to considerable advancement and a better understanding of the device. Some notable developments are-

- Increasing the tuning range by changing the length of the smooth wall waveguide [Moreland *et al.* (1996)]
- Pre-bunching electrons with a resonant reflector increase output power and efficiency [Gunin *et al.* (1998)]
- To enhance efficiency, even more, a non-uniform slow-wave structure (SWS) is used [Wen *et al.* (2000)].
- Using a specifically developed electron beam collector, operate a 100 Hz repetition rate with 1.1 GW of power at 9.38 GHz [Chen *et al.* (2002)]
- To improve velocity modulation, two uniform SWSs separated by a drift tube have been used [Zhang *et al.* (2004)].

- Using two RRs to increase the pulse length [Song *et al.* (2011)]
- Used a trapezoidal resonant reflector to move the peak electric field towards the Centre of the RR, minimizing the likelihood of RF breakdown. [Cao *et al.* (2014)].

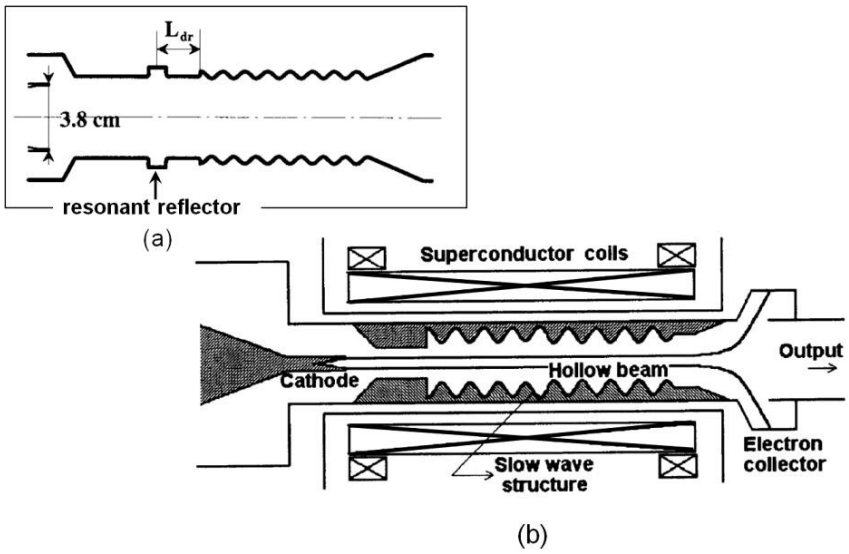

Figure 1.4: Schematic diagram of RBWO (a) with resonant reflector [Guinn *et al.* (1998)], and (b) with electron collector [Chen *et al.* (2002)].

1.3.3 Virtual Cathode Oscillator (VIRCATOR)

A dense cloud of electrons is accelerated against a metallic grid or anode foil in a vircator [Chittora (2016)]. The virtual cathode oscillator (VIRCATOR) [Sullivan *et al.* (1983)] is a specialized HPM source. The beam-wave interaction does not generate microwave radiation in this case. The three geometrical configurations for VIRCATORs are axial, coaxial, and reflex triode [Davis *et al.* (1990)]. Due to the low electrostatic potential, a virtual cathode forms, allowing some electrons to flow in the opposite direction. As a result, electrons bounce back and forth between the virtual and physical cathodes. Here, two types of radiation occur: the

virtual cathode itself oscillates at plasma frequency, and the reflexing electrons oscillate at a different frequency. Although VIRCATORs do not require a magnetic field and have very simple and small construction, the main disadvantage is their low efficiency because the two competing radiations do not occur at the same frequency. However, phase and frequency locking have been established [Price *et al.* (1989)], [Sze *et al.* (1990)]. The output power of VIRCATORs exceeds 1 GW in the L and S bands, with an efficiency of less than 10%.

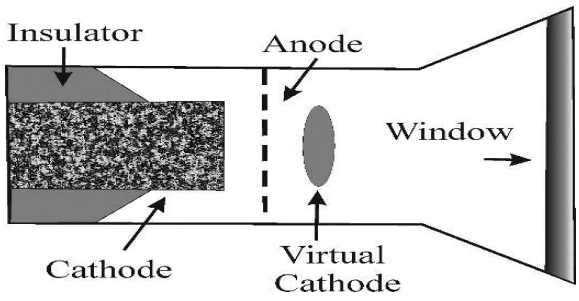

Figure 1.5. Schematic diagram of VIRCATOR [Barker and Schamiloglu (2001)].

1.3.4 Reltron

Reltron is also a new form of high-power microwave (HPM) source capable of generating gigawatts of power at microwave frequencies [Mahto and Jain (2016)]. Its operating principle is the same as that of a klystron, except that it modulates the electron beam twice in modulating cavity and then post-accelerates the bunches toward the extraction cavity with relativistic energy without using an external magnetic field [Benford *et al.* (2006)]. A voltage divider circuit divides the high pulsed DC voltage from the power source and feeds it to the explosive cathode to re-accelerate the highly-dense electron beam and the electron beam entering the RF interaction cavity. In other words, the electron beam is modulated twice in the modulation cavity, the bundle is reaccelerated using the post-acceleration process, and no external DC magnetic field is needed [Benford *et al.* (2006)]. The device predominantly

functions in TM_{01} mode. However, the produced RF is extracted in TE_{10} mode via a rectangular waveguide, therefore, no external mode converter is required. Another Reltron variant based on thermionic emission cathodes has been described for long-pulsed movements of a few microseconds or high energy per pulse [Benford *et al.* (2007)]. Titan Advanced Innovative Technologies in Albuquerque, New Mexico, USA, developed Reltron in 1992. The major benefit of Reltron is that it can produce microwave pulses with a width of nearly one microsecond and hundreds of joules of pulse energy. Apart from that, the frequency-adjustable Reltron can be adjusted ± 10% with respect to the centre frequency [Gold and Nusinovich (1997)]. A typical schematic of the Reltron oscillator is depicted in Figure 1.6. It includes a high voltage pulse, field emissive cathode, modulating cavity, post-acceleration gap, RF extraction cavity, and a beam dump.

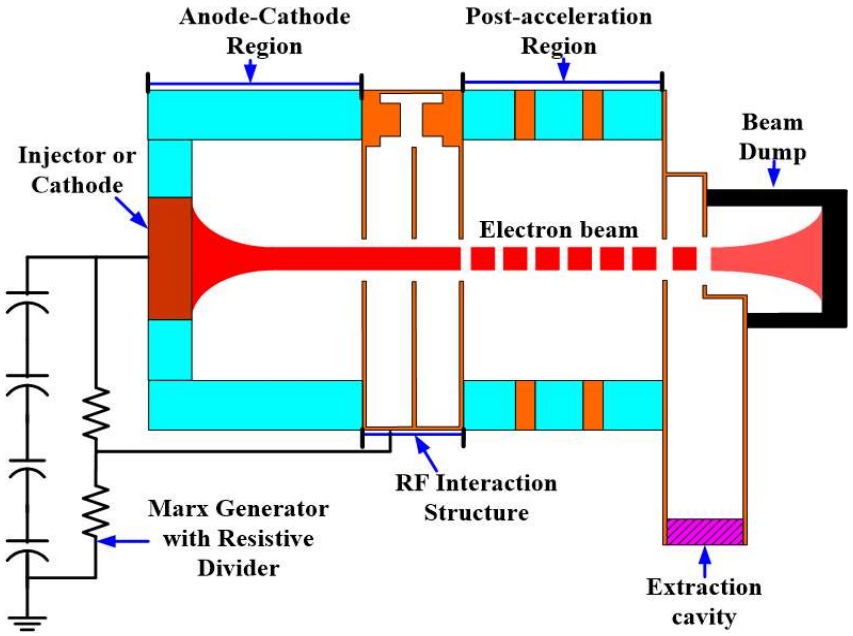

Figure 1.6: Schematic diagram of a Reltron [Miller, R. B., McCullough, W. F., Lancaster, K. T., and Muehlenweg, C. A (1992)]

1.3.5 Arletron

Arletron is a compact HPM source that employs a medium power (1 MW) annular beam to produce HPM with a high repetition rate and long pulse duration (Figure 1.7). The interaction structure is comprised of two pillboxes which are coupled by a beam passage aperture. Here, a small focusing field is provided by the permanent magnet, that's why no power is wasted in external magnetic coils. The device employs the post- acceleration approach to increase output power and minimise energy dispersion in the bunched beam. Through simulation, the arletron produced 350 MW average power at 2.2 GHz with 35% efficiency. It can operate at a very high repetition rate even though it is a griddles tube. It employs tunable plungers to alter the extraction cavity diameter, resulting in a 25% tunability with regard to the central frequency of 2.4 GHz [Gardelle (2009)]. The dimensions of pillboxes and beam characteristics restrict the design possibilities of Arletrons within the 1-6 GHz frequency range. Due to the inadequate focusing field generated by permanent magnets, beam focusing would deteriorate in low-frequency designs. In a high-frequency design, the beam current in a tiny beam dimension would be insufficient to cause bunching. The simulated design was later tested experimentally at the Centre d'Etudes Scientifiques et Techniques d'Aquitaine (CESTA), Le Barp, France [Gardelle *et al.* (2010)]. The experiment employed solid-state pulsed power technology, which provided a 1 kA, 200 kV supply with a repetition rate of 100 Hz and a pulse length of 300 ns. A TEM to TM_{01} mode converter linked to a conical horn antenna radiated the generated microwave, and the radiated power was measured at an 8 m distance using an S-band horn and detector diode.

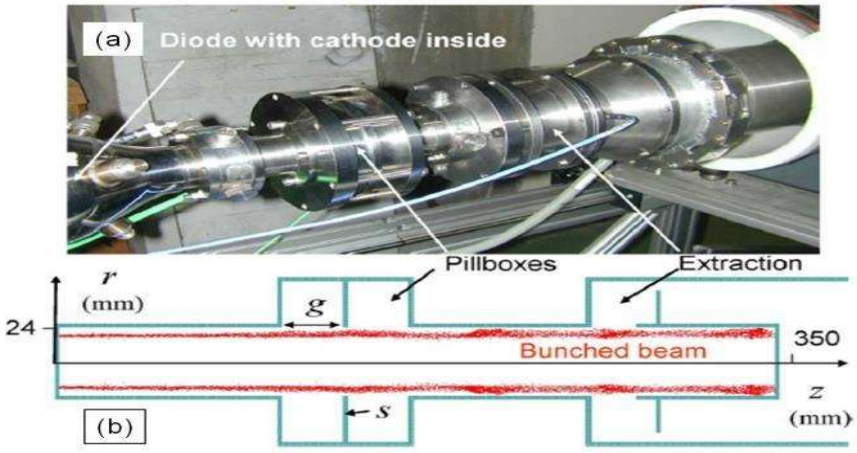

Figure 1.7: Arletron (a) experimental set-up, and (b) MAGIC 3D simulation.

[Gardelle *et al.* (2010)].

1.3.6 Relativistic Gyro Devices

The gyrotron, also known as the "electron cyclotron resonance maser," is a high-power, high-frequency source. The EM wave's phase velocity in the gyro-devices interaction circuit is more than or equal to the speed of light. A magnetron injection gun produces an annular gyrating beam, guided in an open resonator by a high external axial DC magnetic flux generated by a superconducting magnet. The magnitude of the applied DC magnetic flux and the microwave frequency generated from the device are closely associated with the synchronism condition. The cyclotron motion of the electrons within the beam is used to interact with the beam wave inside the cavity, and the transverse kinetic energy of the electrons is turned into an RF wave, leading to the development of a Gaussian wave. After losing their energy, the spent electrons expel from the beam cavity and travel to the collector, where they are finally collected. The actual variation of the gyro-device supported the interaction circuit falls into several categories as per their conventional device counterparts, like, gyrotron oscillator also referred

to as gyro-monotron, gyro-TWT, gyro-klystron, gyro-BWO, gyro-twystron, etc. Fig. 1.8 shows different types of gyrotron devices for their slow-wave and fast-wave.

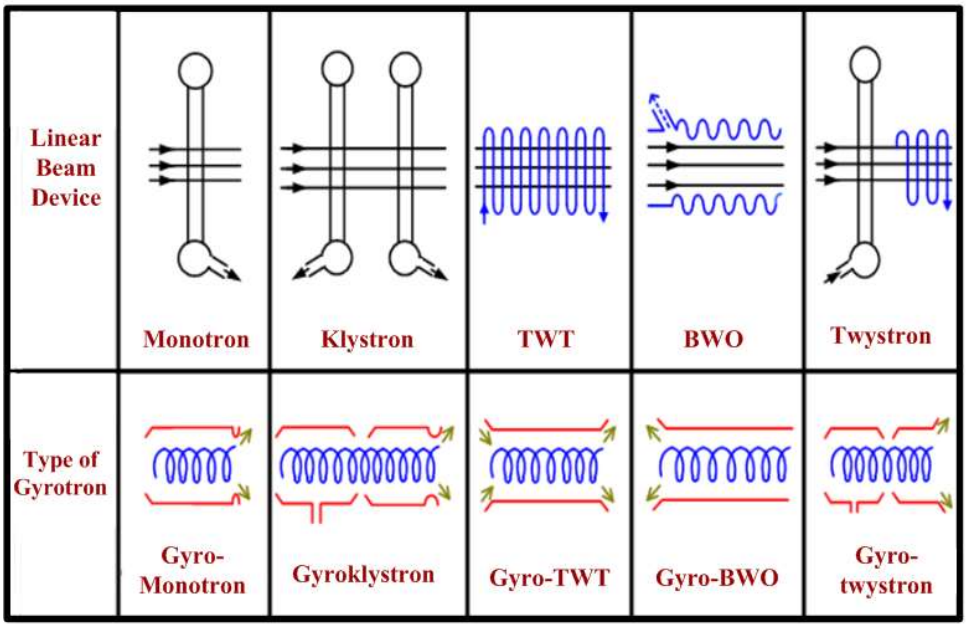

Figure 1.8: All types of Gyro-devices [Gold and Nusinovich (1982)].

1.3.7 Plasma Assisted Slow-Wave Oscillator (PASOTRON)

Similar to BWOs, the plasma-assisted slow-wave oscillator (PASOTRON) uses a cylindrical waveguide with a sinusoidally varying wall radius as SWS (Figure 1.9(a)). A plasma-cathode electron gun generates a plasma that acts as a high-density electron source, with up to 220 kV, 2 kA voltage, and current. While travelling through the lightly ionized plasma channel, the space charge neutralizes the beam. As a result, the magnetic self-pinch force is sufficient to compress the beam, and an external focusing field is no longer required. PASOTRON is a low-weight and compact HPM source that can operate at different frequency bands depending on different SWSs. While it operates in TM_{01} mode, the first reported device has a TE_{11} output mode with fixed polarization. In TE mode, a rotating polarization can also be produced directly. It exhibited extended pulse operation (>100 s) in the C-band with output

power ranging from 1 to 5 MW and a 20% efficiency [Goebel *et al.* (1994)]. PASOTRON was subsequently developed to work as a travelling-wave amplifier in addition to BWO, achieving 20 MW power in long pulses with nearly 1 kJ energy per pulse (Figure 1.8(b)) [Goebel *et al.* (1996)]. In addition, a mode converter was developed to feed power from the helix-PASOTRON to a high-power antenna in TE_{10} mode. The device's desired operation requires vacuum conditioning and tube surface conditioning. The vacuum conditioning eliminates contaminants and surplus gas, allowing the pulse to be longer and more powerful.

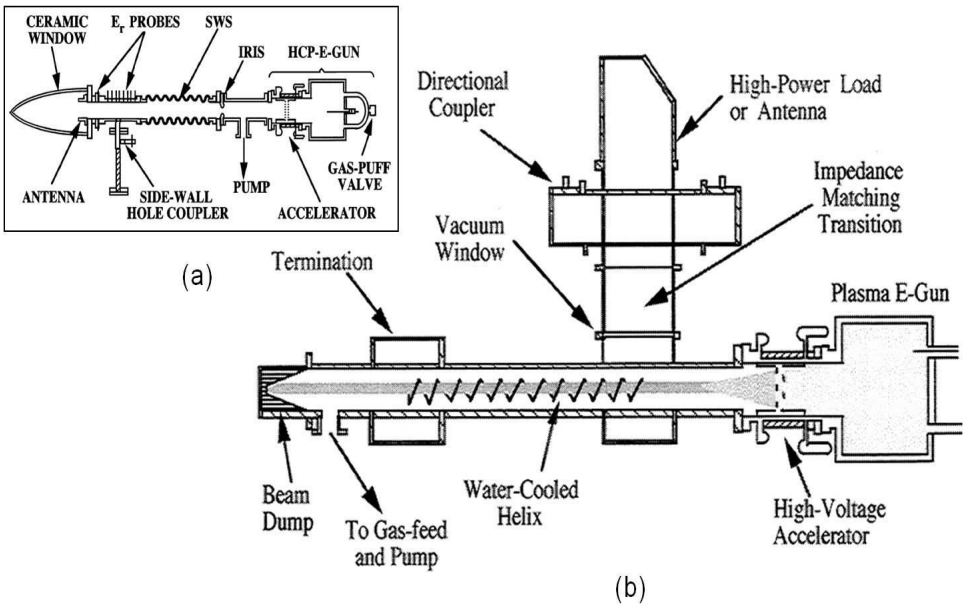

Figure 1.9: Schematic diagram of **(a)** rippled waveguide SWS PASOTRON, **(b)** helix PASOTRON HPM source [Goebel *et al.* (1996)].

1.3.8 Transit-Time Oscillator (TTO)

While passing axially through a high Q cylindrical cavity, an electron beam excites and enhances appropriate electromagnetic modes. In a transit-time oscillator, this phenomenon is

used to generate microwaves. Muller proposed a transit-time effect-based device monotron in 1933 [Muller (1933)]. Due to the lack of relativistic beam technology at the time, the device had a slow growth rate and was exceedingly inefficient. Research in this field was abandoned due to technological imitation for almost six decades. In TTO development, the 20% efficiency in SCO was a notable achievement [Marder *et al.* (1992)]. However, because of the high diode impedance (~100 Ω), the input beam power was limited, restricting the output power. The transit-time amplifier was proposed in 1993 as a high-efficiency narrow-band device requiring a low magnetic field (0.5 KG), and simulation predicted approximately 1 GW power in X-band [Arman *et al.* (1993)]. The radial acceleration (Figure 1.10 (a)) was developed as a low impedance (~25 Ω), repetitively pulsed device with great power capabilities. The simulation predicted 1 GW output power with 50% efficiency [Arman (1996)]. The device's drawbacks were a long saturation time and trouble in extracting output. In 2009, a more promising low-impedance TTO (LITTO) with an annular cathode, coaxial extraction section, and external magnetic field was developed (Figure 1.10 (b)). The interaction structure LITTO is similar to SCO. It uses a dual cavity extractor section that produces higher current modulation. The low impedance TTO would produce 5 GW at 1.6 GHz frequency with 23.1 % efficiency with 600 kV, 36 kA input, and a 0.45 T focusing magnetic field [Cao *et al.* (2009)].

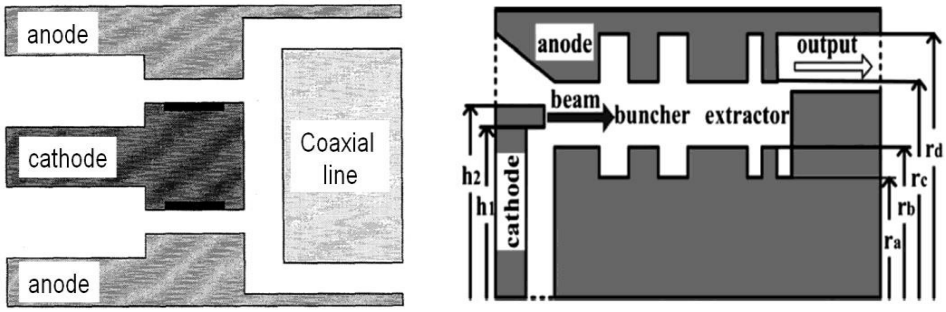

Figure 1.10: Schematic diagram of **(a)** radial acceleration [Arman (1996)], and **(b)** low impedance TTO (LITTO) [Cao *et al.* (2009)].

1.3.9 Split Cavity Oscillator (SCO)

A conducting screen divides a pillbox cavity symmetrically into two pillboxes in a split cavity oscillator (SCO), allowing an electron beam to pass through with minimum interception (Figure 1.11). The screen is positioned so that there is a space between it and the outer cavity wall. Along with the conventional modes, this arrangement gives rise to a new category of cavity modes in the interaction region. The SCO mode (the basic mode of this new kind) rises in amplitude due to an unstable interaction with a traversing electron beam, which takes the beam's kinetic energy. When the field amplitude reaches saturation, it is large enough to bunch a traversing beam. Thus, it fully modulates a large cross-section beam within a small distance without any focusing arrangement, overcoming the space-charge and pinching limitations [Marder *et al.* (1992)]. The SCO was developed from the need for a long pulse microwave tube with high power capability. The two needs were accomplished with a long pulse duration (typically 1 μS), and achievable phase-locking of several oscillators to attain high total power. For an applied voltage, the simulation results show that if the beam current is much lower than the Child-Langmuir current, the oscillation is weak and dominated by the second harmonic. For fundamental mode operation, the screen spacing should cause approximately the same emission as the Child-Langmuir current.

An inverse diode collects the bunched beam and creates a coaxial transmission line with the interaction section's extended outer wall. An iris opening extracts the microwave, which changes the coaxial transmission line into a cavity with an appropriate Q and resonant frequency. For a successful extraction, the iris must be properly positioned. SCOs can be made in different shapes, including pillbox, elongated, and annular. The SCOs have a voltage range of 100-300 kV and an impedance range of 50-100 Ω. Over an 800 nanosecond pulse period,

investigations showed 25 MW of average radiated power with an efficiency of 8% (almost twice peak power and efficiency). The efficiency can be enhanced by using the post acceleration technique, and the power can be improved by using annular beams with a large area or by phase-locking multiple devices. Up to five SCOs were successfully phase-locked.

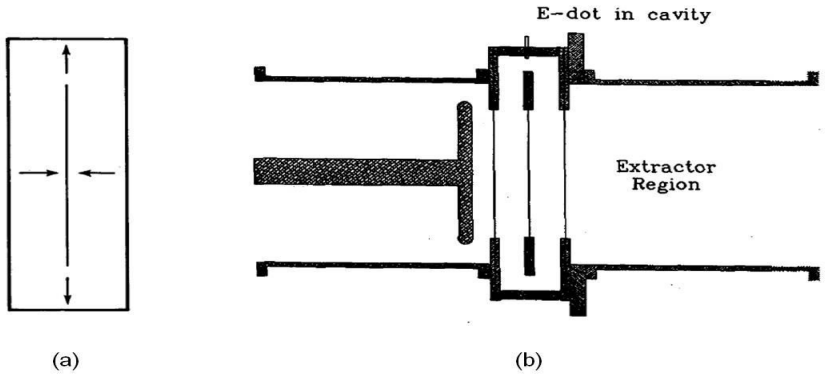

Figure 1.11: SCO **(a)** fundamental mode, and **(b)** schematic of experiment [Marder *et al.* (1992)].

1.3.10 Relativistic Magnetron

A magnetron is a cross-field device, which is basically a diode with a magnetic field perpendicular to the applied electric field. The magnetron is the first developed microwave device. Magnetrons were produced on a massive scale during WW II, "and magnetron-driven radar had a larger impact on the war than any other technology developed in World War II, even more than the atomic bomb." The electrons drift with a velocity close to v_{ph} of the slow electromagnetic wave in the interaction region. A cylindrical magnet's operating voltage is found using the Buneman–Hartree resonance condition, while the Hull cut off condition determines the magnetic field range. Interaction space refers to the area between the cathode

and the anode where the electron beam and wave interact. The electrons are released from the cylindrical cathode surface because of the explosion of the microprotrusions when a DC accelerating voltage is provided between the anode and the cathode. The electron will be unable to reach the anode if the field is sufficient enough [Benford *et al.* (2006)]. The Brillouin layer refers to the electron cloud. The space charge drifts velocity will reduce when the axial external magnetic field (B_Z) is moderately raised beyond B*(at a constant voltage V) critical magnetic field. Strong oscillations in the mode will then terminate [Benford *et al.* (2006)]. The Buneman-Hartree condition determines the magnetic field $B_Z = B_H$ for which this occurs. Buneman-Hartree voltage is the voltage at which, when oscillations are provided at the same time magnetic field is ample enough so that undistorted space charge does not stretch out to the anode.

The applied DC voltages and currents figure out the difference between an ordinary magnetron and a relativistic magnetron [Benford *et al.* (2007) and Chandra *et al.* (2014)]. A relativistic magnetron is a stable, compact, and efficient HPM source, and the depth of the anode cavities determines its oscillation frequency, making it difficult to tune during operation [Benford (2010)]. The two main modes of relativistic magnetrons are the –π mode, in which neighbouring cavities are out of phase, and the 2π-mode, in which each resonator has the same field pattern. [Benford *et al.* (2006)] clearly explain the electric field structure of the π - and 2π-modes of an A6 relativistic magnetron. The A6 relativistic magnetron is one of the most popular, and much literature work has been done. This magnetron's resonant structure consists of six cavities with a 60-degree azimuthal spacing. The cathode radius is r_c, whereas the anode radius is r_a. The radius of the vane is r_w, and the angles subtended by the cavity at the centre are ψ. Figure 1.12 is the cross-sectional view of the A6 relativistic magnetron.

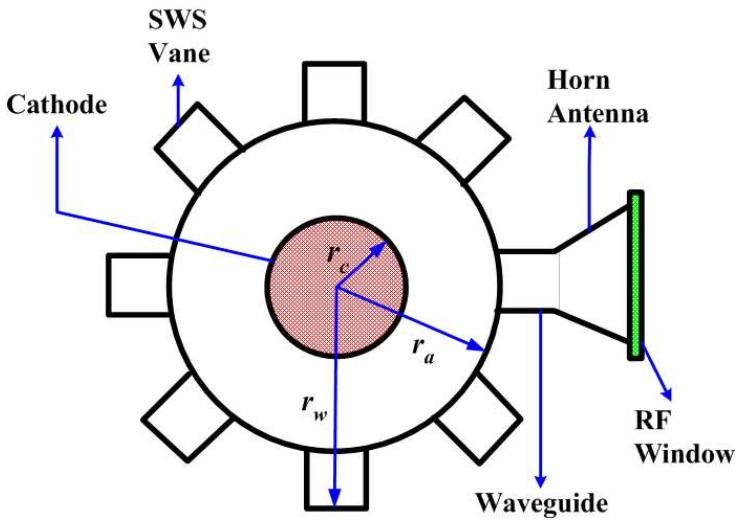

Figure 1.12: The typical schematic view of relativistic Magnetron [Bekefi *et al*. (1976)].

1.4 Magnetically Insulated Line Oscillator (MILO)

Microwave oscillators that do not need an external DC magnetic field have been the subject of intensive research. Microwave oscillators that require an external magnetic field use two DC power sources to achieve magnetic insulation, but electrical breakdown occurs when higher voltages are approached. The intrinsic impedance of these oscillators is quite high, significantly restricting the power level at which they can operate. Thus, for efficient operation at greater power levels, an oscillator with lower impedance would be preferable, eliminating the problem of voltage matching [Bekefi *et al.* (2006)]. To overcome the above problems, a Magnetically Insulated Line Oscillator (MILO) has been used, which is an efficient and compact high-power microwave source. The main benefit of this device is that an external magnetic field is not needed for magnetic insulation and has a very low impedance, allowing it to function at greater power levels. MILO makes the device more compact and lightweight by

supplying the desired magnetic field with the help of the electron beam current itself instead of using a separate magnet. Table 1.2 shows a comparison of MILO to various HPM sources.

Table 1.2: Comparison of MILO with other HPM Sources.

Parameters	**RK***	**RBWO$**	**RM#**	**Reltron**	**Vircator**	**MILO**
Osc. or Amp.	Osc./ Amp.	Osc.	Osc.	Osc.	Osc.	Osc.
Efficiency	35-60 %	40 %	20-30 %	30-40 %	1 – 3 %	20-30 %
Operating Frequency	Up to *Ku*-band	Up to *Ku*-band	Up to *Ku*-band	Up to *X*-band	Up to *X*-band	Up to *Ku*-band
External Magnetic field Required or not?	Yes	Yes	Yes	No	No	No
Construction complexity	Easy	Easy	Complex	Complex	Easy	Easy
Size	Heavy	Heavy	Heavy	Heavy	Compact	Compact
Impedance	High	High	High	High	Low	Low
Oscillation mode	TM_{01}	TM_{01}	TM_{01}	TE_{10}	TM_{0n}	TM_{01}
Input voltage changes, Frequency oscillation changes?	No	Yes	Yes	No	No	No

* Relativistic Klystron
$ Relativistic Backward Wave Oscillator
\# Relativistic Magnetron

The schematic structure of Load-Limited MILO is shown in Figure 1.13. It comprises a coaxially loaded metal disc as a slow-wave structure (SWS) with an explosive emission cathode on the inner conductor, a filter or chokes cavity on the input side, one extractor cavity on the output side, an inductive stub, and a collector.

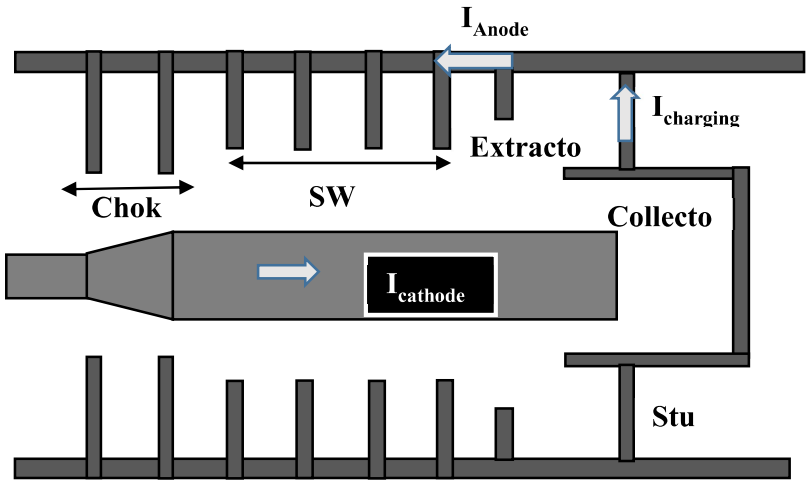

Figure 1.13: The typical schematic view of a Load-Limited magnetically insulated line oscillator (MILO).

1.4.1 Sub-Assembly Description of MILO

The major sub-assemblies of a MILO are (i) Cathode, (ii) Choke cavity, (iii) RF interaction structure, (iv) Extractor cavity (v) Beam Dump.

a) **Cathode:** It's an important sub-assembly that generates a proper electron beam for RF wave interaction. MILO is a gigawatt class device that requires an explosive emission cathode because such cathodes "turn on" at relatively fewer electric fields and supply the very large current densities of 100`s of A/cm^2 that allow the tube to generate an excessive rise in RF power. The device's cathode surface is often covered with velvet for explosive electron emission (EEE) because it is less costly and has a low electric field threshold (1kA/cm), and a low plasma closure velocity [Adler *et al.* (1985), Miller (1998)]. The cold cathode follows the law of field emission when subjected to a high electric field. When an electron gains enough potential energy through growing temperature or a strong electric field, it breaks and is released into the vacuum. The

potential difference between the cathode and the anode accelerates this process. The velvet cathode's light emission mechanism is depicted in Figure 1.14.

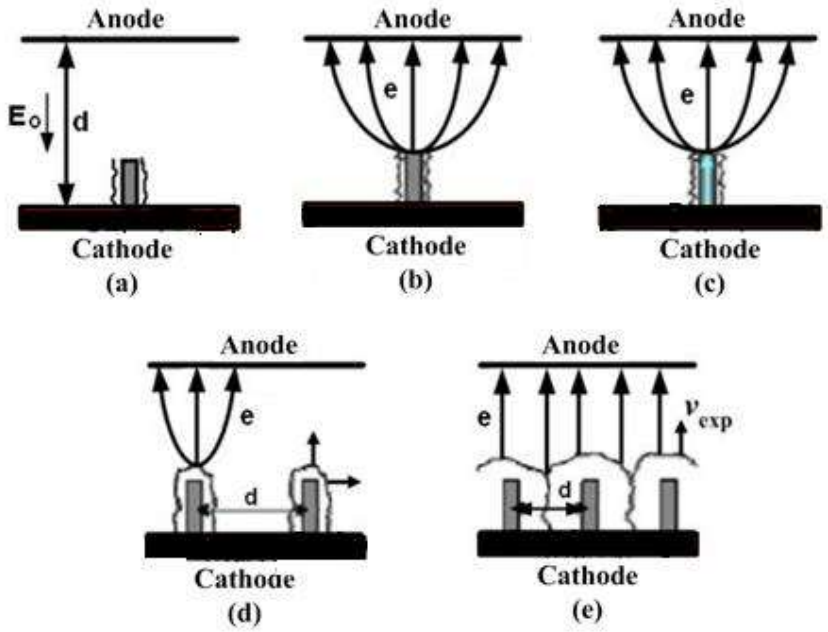

Figure 1.14: Process of electron emission from a velvet surface: (a) the application of the intense electric field causes the partial destruction of fibre and the creation of a dense plasma column. (b) Electrons are emitted from plasma and form a space charge current of the Child-Langmuir type. (c) Heating occurs in fibre due to the Joules effect. (d) Expansion of the plasma column at the thermal speed, and (e) Reduction of inter-electrode space by the total expansion of the plasma of the cathode [Miller (1998)].

A variety of cathodes can be used instead of velvet cathodes. When the electric field surpasses 20 kV/cm, dielectric fibre is used as the cathode, triggering the surface flashover process [Miller (1998)]. In terms of lifetime and shot-to-shot repeatability during repeating rate operation, the graphite cathode beats the velvet cathode and acts as a favourable cathode for the MILO device for repetitive rate conditions. Carbon fibre cathodes impregnated with caesium iodide (CsI) salt have proved to be superior to regular velvet cathodes in terms of performance.

It has advantages, including being lightweight and requiring no heater for electron emission. MILO has also proposed a metal-dielectric cathode to enhance its pulse repetition rate and maintenance-free longevity [Fan et al. (2008)]. Metal array cathodes (MACs) are now used in MILO devices. It has a greater lifespan and a much-lessened repeat rate than Velvet, representing a promising approach to MILO repeat operations [Qinetal *et al.* (2016)].

b) **Choke Cavity:** MILO devices use a periodic disc-mounted coaxial structure in which the first few discs form a choke cavity. The choke cavity mainly serves as a low pass filter, preventing RF leakage to the input DC source. It also serves as an in-phase reflector, improving the interaction of beam waves while lowering the load on the DC pulse power source. Due to the impedance differential between the rearmost choke disc and the foremost primary disc, the electron flow in the primary SWS moves closer to the cavity hole where the RF voltage is maximum. This leads to a rise in power conversion efficiency. At low impedance, increased current exists in the electron flow, resulting in increased power available for microwave generation. The first experimental prototype developed by the US Air Force in Cart land did not have this chalk [Lemke and Collin (1987)].

c) ***RF Interaction Structure or Slow Wave Structure (SWS) Cavity*:** MILO is a slow wave RF interaction structure made up of a series of coaxial metal discs. The disk cycle forms a cavity. In basic TM mode, the interaction cavity oscillates. Each cavity acts as a 1/4 wavelength oscillator out of phase with the next cavity in this mode. Therefore, the RF interaction cavity oscillates in π mode, which can store large electromagnetic energies, rather than in propagation mode.

d) ***Extraction Cavity:*** The extraction cavity design significantly impacts MILO output. The extractor portion consists of the last MILO vane (i.e. extractor vane) and the axial

distance between the extractor vane and the coaxial transmission line (called the extractor gap). The extractor vane's inner radius is slightly bigger than the rest of the vanes to supply an adequate impedance match between the extractor gap electric field and the output coaxial transmission line's electric field (CTL). The extractor turns the standing wave into a travelling wave that can propagate outside.

e) ***Beam-Dump/Collector*:** For an effective impedance match of the extractor gap to the output coaxial transmission line, the radius of the extractor vane is similar to the outer radius of the beam dump. In order to extract RF energy, the extractor cavity must be coupled to the output waveguide. Because the radial component of the RF electric field is highest on the internal radius of the extractor vane, the radius of the extractor cavity is the same as the external radius of the beam dump but larger than the interaction cavities. The radial component on the vane tip is directly attached to the output coaxial transmission line. The covering of the collector on the cathode constitutes an additional cavity that stores the RF energy generated in the MILO and then transfers this energy to the external load in pulse form.

1.4.2 Principle of Operation

The MILO works on the relativistic flow of electrons inside a coaxial magnetically insulated transmission line that is loaded with a slow wave structure, generally thin metal vanes. The geometry of MILO is the same as that of a linear magnetron or crossed- field amplifier. A MILO operation is divided into four basic stages, which start with the emission of electrons from the cathode surface, then the magnetic insulation condition attained by the device, followed by noise formation and beam-wave interaction, and finally ends with the withdrawal of RF energy out of the device.

Electron emission: The high-potential UHF pulse device is applied between the cathode and anode. The distributed electron emission from the cathode surface is enhanced due to the potential difference between the cathode and anode in this device.

Magnetic insulation: The critical current is the smallest amount of current required to initiate the self-magnetic field that creates insulation between the anode and cathode. Because of the self-magnetic field created by the anode current when it exceeds a critical current, all electrons are confined between the anode and the cathode. This is the core concept of MILO which generates extremely high-power microwave pulses. The load current regulates the device's magnetic cut-off and interaction conditions. The distance between the collector and the cathode determines the value of the load current.

Noise formation and Beam-wave interaction: Electron velocities and charge density in the streaming space-charge cloud swing randomly with respect to time due to variations in the emission process and noise-amplifying influences inside of space-charge Hub (Beam current) between cathode and anode, producing a noise constituent of the beam current in the space charge hub. The fluctuation of frequency varies so widely that the noise is known as "white noise," which indicates fluctuations with an unlimited frequency range. While the frequency range of fluctuations is not limitless, it is rich in microwave components, therefore, there are components present to initiate any of the frequencies that the SWS cavity of MILO can handle. The hub's noise current generates noise current inside cavities. When the resonant frequency constituent of the noise current goes across a large impedance of the cavities at one of the resonant frequencies, the RF voltages are generated over the cavity gaps, amplifying the RF current inside of the hub. When the power provided to the MILO is equivalent to the power to the load with the addition of losses, the RF current and power rapidly grow and saturate. Whenever the synchronism condition is arranged such that the axial velocity of the electron

flow is similar to the phase velocity of the RF waves in the anode SWS, then it helps in the formation of the electrons bunches, and the energy of the retarded electrons is transferred to the RF waves.

The MILO device is made up of more than three interaction cavities that oscillate in their fundamental mode (i.e. in π -mode). The phase difference between these interaction structure cavities is 180 degrees, and they behave like a quarter-wave oscillator. The highest electric field occurs at the tip of the disc, and the highest magnetic field exists at the top of the cavity in the π -mode, resulting in a spoke-like structure within the device. The produced electron spoke is majorly accountable for the device's beam-wave interaction, and the electrons finally lose their potential and kinetic energy to the electromagnetic field. The generated RF signal is stored as a standing wave with a group velocity close to zero in the interaction structure. The extractor portion is responsible for extracting the cavity's stored energy.

RF Extraction: The RF energy is stored in the SWS cavities as a standing wave, which is extracted using an extractor cavity. By slightly changing the group velocity of stored RF energy, the extractor mainly converts the standing wave into a travelling wave

Thus the whole working mechanism of the MILO device can be explained in the flow chart given below:

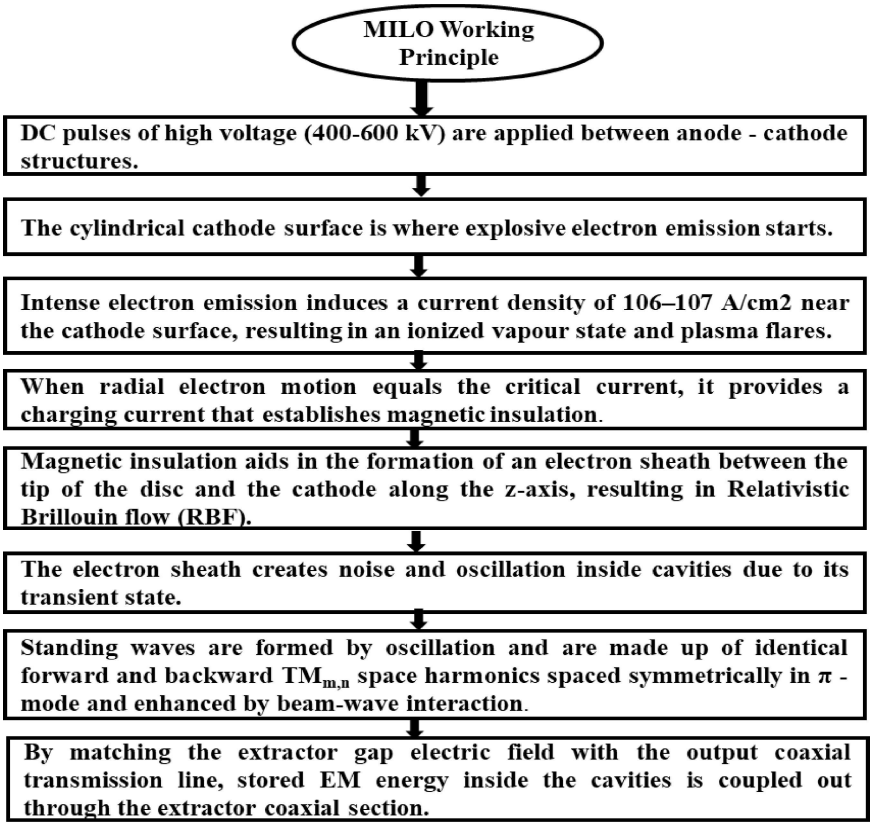

Figure 1.15: Flow chart of the working mechanism of MILO

1.5 Literature Review on MILO

1.5.1 MILO Development TimeLine

Table 1.3 shows a literature review in the development field of MILO design and its technological improvements for overall performance enhancement.

Table 1.3: Chronological order of development of MILO device.

Year	Title	Author/Lab	Frequency	Input Voltage/ Current	O/P power/ Rep. rate	Efficiency
1997	Load-Limited MILO	R. W. Lemke *et. al.*/ USAF Lab	1.18 GHz	510 kV, 34 kA	1.35 GW, Single shot	7.7%
1998	Pulse lengthening multi GW MILO	M. D. Haworth *et. al.*/ USAF Lab	1.2 GHz	500 kV, 60 kA	1.875 GW,	6.6%
1998	The Tapered MILO	J. W. Eastwood *et. al.,*	1 GHz	440 kV, 30 kA	1.35 GW	10.5%
2007	Compact MILO	R. Cousin *et. al.*/ LPTP France	2.4 GHz	500 kV, 45 kA	1.35 GW	6%
2007	Improved MILO	Y. W. Fan *et. al.*/	1.74 GHz	550 kV, 57 kA	2.4 GW	7.6%
2008	Giga watt MILO	D. H. Kim *et. al.*	1 GHz	466 kV, 34 kA	1.82 GW	11.5%
2008	Improved MILO with the high rep. rate	Y. W. Fan *et. al.*	1.755 GHz	510 kV, 54 kA	2.17 GW With 20 Hz rep. rate	7.9%
2008	X-band MILO	Y. W. Fan *et. al.*	9.7 GHz	400 kV, 50 kA	110 MW, Single shot	>1%
2009	S-band Tapered MILO	M. D. Li Zhi-Qiang *et. al.*	2.63 GHz	500 kV, 35 kA	2 GW,	11%

2009	Bi-Frequency MILO	Dai-Bing Chen *et. al.*	1.26 GHz & 1.45 GHz	420 kV, 34 kA	620 MW	4.2%
2013	*Ku*-Band MILO	Jie-Wen *et. al.*	12.9 GHz	539 kV, 57 kA	89 MW	>1%
2015	Metal Dielectric cathode MILO	Xiaoping Zhang *et. al.*	1.562 GHz	425 kV, 34 kA	1.95 GW	13.5%
2015	Improved Ku- band MILO	Tao-Jiang *et. al.*	13.02 GHz	450 kV, 45 kA,	150 MW	>1%
2015	Complex dual-band HPM source	Xiaoping Zhan *et. al.*	MILO-2.1 GHz and VCO-3.8 GHz	440 kV, 35 kA	MILO-1.7 GW VCO-0.37 GW	13.4%
2016	High efficient rep. pulsed MILO	Yu-Wei Fan *et. al.*	1.598 GHz	420 kV, 40 kA	2.1 GW, With 5 Hz	15.5%
2016	MILO with metal array cathode	Fen Qin *et. al.*	1.56 GHz	544 kV, 60 kA	2 GW	6.3%
2016	Tunable MILO	Yu-Wei Fan *et. al.*	1.337-1.760 GHz	430 kV, 40.6 kA	1.51 GW-2.653 GW	8.7-15.2%
2017	Carbon fibre array cathode HTMILO	An-Kun Li, Yu-Wei Fan, and Bao-Liang Qian	1.56 GHz	460 kV, 48 kA	2.9 GW	13.1%
2017	Vacuum-sealed repetitively pulsed MILO	Tao-Xun *et. al.*	1.58 GHz	630 kV, 48 kA, Rep-rate: 5 Hz	3.4 GW	11.24%
2017	Ku-band MILO with	Tao- Jiang *et. al.*	12.36 GHz	515 kV, 48 kA	1.2 GW	4.85%

	Tapered choke cavity					
2019	Ridged Disk-Loaded MILO	Xiaoyu Wang *et. al.*	1.48 GHz	566 kV, 50 kA	6 GW	21% (Simulation)
2020	Novel High-Efficiency MILO	Xiaoyu Wang *et. al.*	1.42 GHz	586 kV, 49 kA	6.3 GW	22% (Simulation)

1.5.2 Literature Review

The first significant work for the magnetically insulated line oscillator (MILO) in high-power microwave generation was reported by Clark et al. in 1988. The different MILO configuration with geometries such as planar, coaxial, and concentric were used and is shown in Fig. 1.16. The experiment was performed with 400kV voltage, 50kA current, and 50 ns pulse width. They observed MILO simulation at the 1.5GHz frequency having 10% efficiency. In 1995 Ashby et al. performed the experiment and simulation of L- band MILO at 1GHz frequency with 500kV voltage and 21kA current and further reported 10.8 efficiencies.

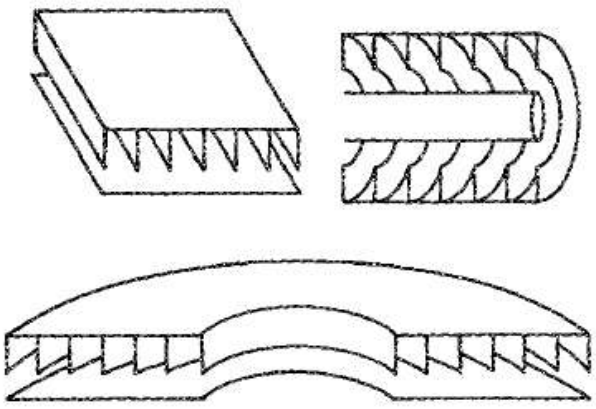

Figure 1.16: Different MILO configurations [Clark *et al.* (1988)].

In 1997, Lemke *et al.* used numerical simulation to examine a non-linear regime in a load-limited MILO, taking power conversion efficiency restrictions into account. They suggested different theoretical aspects for spokes formation, load-length calculation and efficiency estimation for the load limited MILO device. The MILO's dc operating characteristics were discovered by a current-carrying load included in a unique power obtaining scheme. The power is maximized in case the RF choke is utilized with regard to the upstream boundary. The RF choke surges output power by two basic techniques: 1) it contributes to maximum feedback by reflecting the backwards-propagating waves, and 2) it raises the downstream spoke current. They concluded that the PIC Simulation of L-band MILO provided an output power of 3 GW for 493 kV, 56.2 kA, having an efficiency of 10.8%. In 1998, Haworth et al. continued the above experiment with the objective of major pulse lengthening. Because of the spurious electron emission and asymmetry in a MILO design, the MILO device has a pulse shortening problem [Agee *et al.* (1996)]. Haworth et al. built an entirely stainless steel, brazed version of the tube using Hard-Tube MILO (HTMILO), as shown in Fig. 1.17 and achieved a 25% increase in output power and a two-and-a-half-fold increase in RF pulse duration.

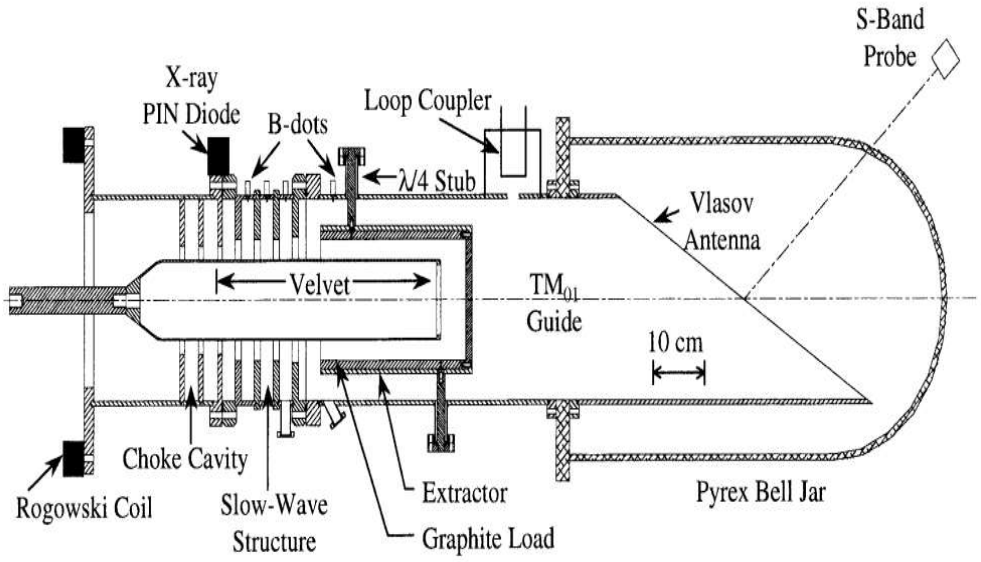

Figure 1.17: Configuration of Hard-tube MILO (HTMILO) [Haworth *et al.* (1998)].

Eastwood *et al*. presented a new MILO design in 1998, which featured a tapered SWS structure, a diode layout, and axial power extraction. Through simulation and experimentation, they attained a 20 per cent efficiency in the L-band. The tapered SWS structure, tapered multi-extractor cavity, and diode gap are the major features of this device. The diode gap primarily controls the load current and contributes to the device's self-magnetic insulation. A tapered SWS structure aids efficient beam-wave interaction, and a tapered extractor cavity gradually increases the group velocity of RF generated and stored in SWS cavities, resulting in this device's high efficiency. The configuration of Eastwood *et al.* is shown in Fig. 1.18.

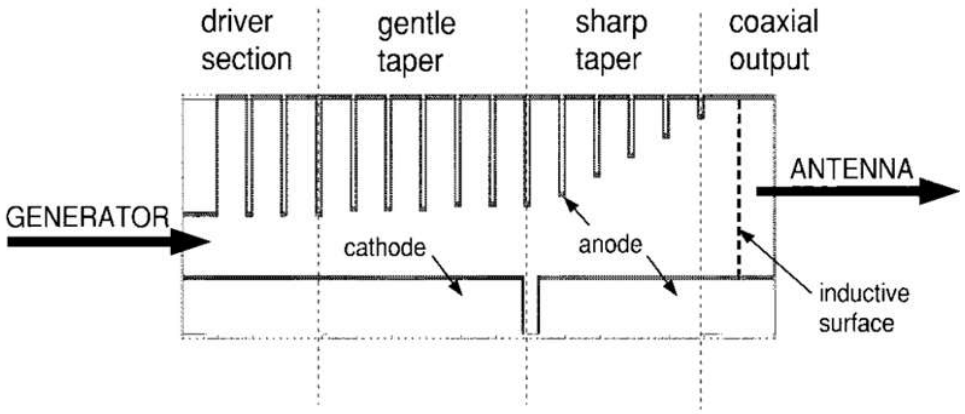

Figure 1.18: The configuration of tapered MILO [Eastwood *et al.* (1998)].

In 2000, Bao-Liang Qian et al. showed a 2D analysis of relativistic para potential electron flow in the MILO, in which distribution expressions for velocity and energy were derived along with expressions for density, the self-electric and self-magnetic fields of electron flow were also obtained, and numerical analysis was performed for each of them.

Haworth *et al.* developed an improved cathode design for long-pulse MILO functioning in 2001, which increased the emitted microwave pulse duration from 200 to 400 nanoseconds. This was accomplished by increasing emission homogeneity in the cathode's launch point region, which reduced anode plasma production. In 2005, Fan *et al.* developed compact MILO with a new beam dump type. The enhanced MILO model included a novel beam dump, a one cavity RF choke section, and a novel mode-transducing antenna. The PIC KARAT code was used to examine the improved L-band MILO with RF power of 2 GW at voltages of 520-540 kV and currents of value 58-62 kA.

In 2007, Richard Cousin et al. developed a gigawatt class of MILO powered by a low-impedance Marx generator. An in-vacuum antenna and a far-field horn are used to confirm the working frequency of 2.40 GHz. The MILO's frequency response was compared to a 3D

simulation done with MAGIC. The first experiment yielded a three microwave of 1 GW output power, which agrees well with the simulation results.

In 2007, Fan Yu-Wei *et al.* presented a dual-band high-power microwave source to improve MILO's power conversion efficiency. Figure 1.19 depicts a typical double band HPM source MILO arrangement. To use current in the MILO, an axially extracted virtual cathode oscillator (VCO) was added. It is known as the MILO-VCO arrangement, in which both are synced to generate HPM. The MILO-VCO was simulated using the KARAT code, and the output power was 5.22 GW with a 16.3% efficiency. The MILO was having a maximum power of 3.91 GW at 1.76 GHz, and the peak power for VCO is 1.33 GW at 3.79 GHz in this MILO-VCO combo.

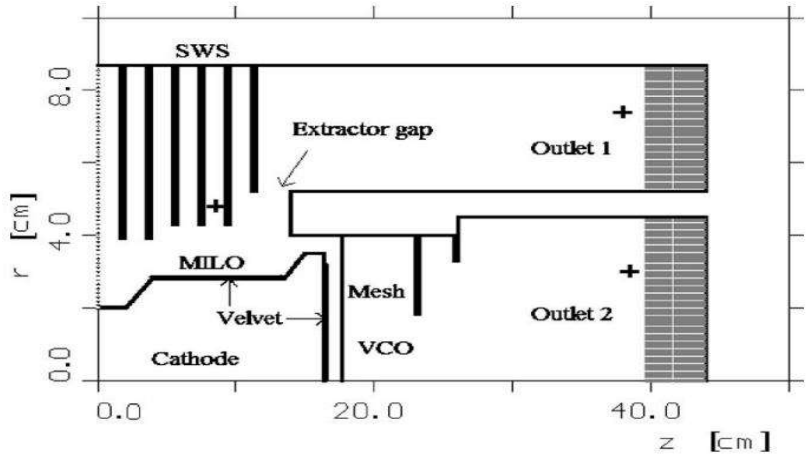

Figure 1.19: The configuration of MILO-VCO [Fan *et al.* (2007)].

In 2009, Jin-Chuan Ju *et al.* studied an innovative dual-frequency MILO having two independent, balanced, and pure HPMs. Figure 1.20 depicts the design's configuration of dual-frequency MILO that are MILO-1 in the C-band and MILO-2 in the X-band, respectively. In accordance with the simulation results, when an electron beam having a voltage of 610 kV and

a current of 82 kA drives the dual-frequency MILO, the two high-power microwaves (HPMs) that are formed have 5.9 GW total power and a power conversion efficiency of roughly 12%. MILO-1 produced 3.2 GW of power at 7.6 GHz, and MILO-2 produced 2.7 GW of power at 9.2 GHz. Two advantages of the suggested dual-frequency MILO are (a) high efficiency and (b) frequency adaptability.

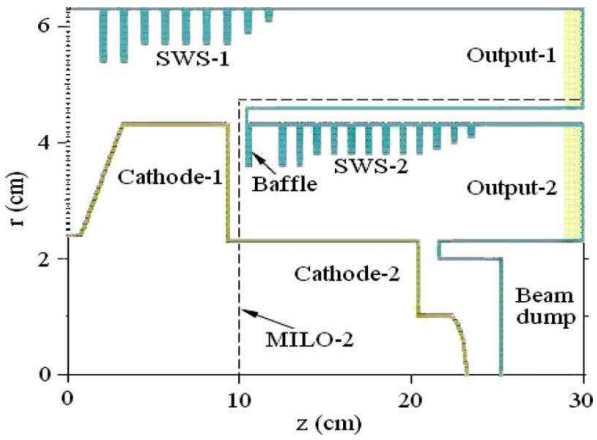

Figure 1.20: The illustrative image of the dual-frequency MILO [Ju *et al.* (2009)]

In 2009, Dai-Bing Chen *et al*. developed a bi-frequency (BF) MILO that utilized a novel azimuthal partitioning concept to create HPM at two frequencies of 3.4 GHz and 3.65 GHz in a single device. Figure 1.21 shows the bi-frequency MILO arrangement. The difference in amplitude in the spectrum between the two microwaves is about 0.4 dB. This MILO was created by azimuthally modifying the depth of the cavity of a conventional MILO while keeping the self-insulated current, total anode current, and total impedance the same as a typical MILO. The output power of the simulated C-band BFMILO was stable at 1.43 GW for 490 kV, 45 kA, with a power conversion efficiency of 6.5 %.

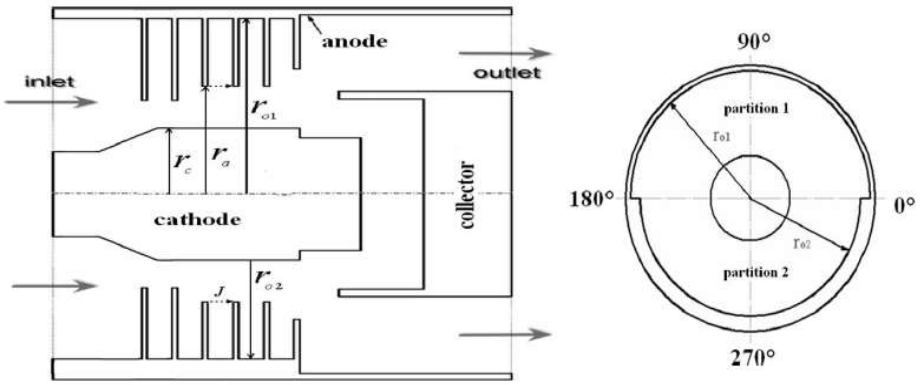

Figure 1.21: Bi-frequency MILO configuration: (a) axial view, and (b) front view.

Extensive theoretical work has been carried out related to MILO device, including the analysis of their interaction structure with the absence and presence of an electron beam. In 2010, Wang et al. studied the periodic disc-loaded coaxial structure with azimuthal partition using field matching theory.

Dwivedi and Jain in 2013, optimized and enhanced the RF characteristics of the S-band MILO using MAGIC PIC code for 600 kV, 35 kA. The developed MILO device was analyzed for the designed value of voltage 600 kV, current 35 kA, and obtained 1.0 GW of RF output power with a power conversion efficiency of ~6% for the common design parameters. The optimised S-band MILO structure produced an output power of 2 GW. In 2016, Dixit et al. performed an analogous circuit investigation for disc-loaded coaxial structures with azimuthally symmetric TM_{0n} modes.

In 2017 Dixit *et al.* presented a design advancement for the rise in the efficiency of L-band MILO. Through simulation, they reached the highest power conversion efficiency of 22.4%. In 2017, Nallasamy et al. demonstrated an electromagnetic simulation in addition to experimental characterization for the RF interaction structure of an S-band MILO.

They performed a cold test of the RF interaction structure with the help of the 'CST studio suite', which was confirmed through the experiment. In 2019, Kumar *et al.* has done the performance improvement of MILO by using an equivalent circuit approach and achieved an RF output of 1.38 GW with 7.8 % efficiency. Kumar *et al.* used the azimuthally partitioned cathode structure in MILO by which MILO operate at two different frequency of L band and analysis have done by the equivalent circuit approach in beam absent and beam present case both in 2020.

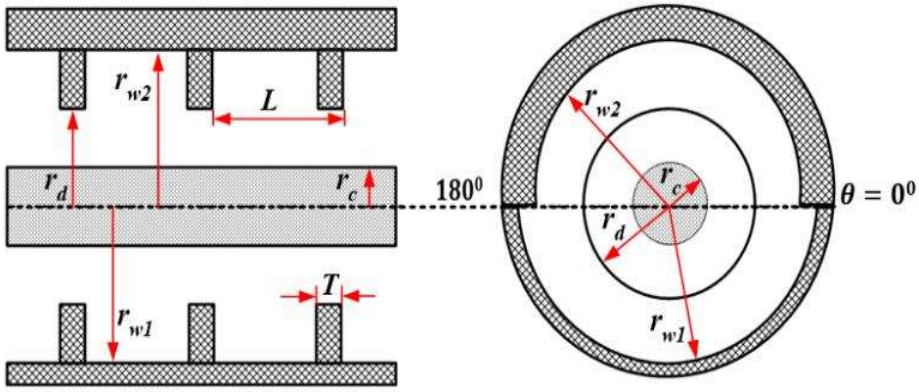

Figure 1.22: Illustrative figure of an azimuthally partitioned axially periodic metal disk-loaded coaxial structure. (a) Sectional view. (b) Front view.

Wang *et al.* proposed the high-efficiency MILO in which they changed the width of an extractor, SWS cavity, and Vane to achieve an efficiency of 22 % at 1.42 GHz with 586 kV of voltage and a current of 49 kA in the year 2020. Wang et al. designed the ridged disk vane MILO (RMILO) and performed the experiment by applying 486 kV voltage and the 51 kA current, then 2.9 GW of peak microwave power is achieved having a pulse duration of greater than 35 ns and a microwave frequency of nearly 1.48 GHz in the year 2021. Under the same conditions, the RMILO's power efficiency increases to 11.7 per cent, a 25 per cent gain over the CMILO.

1.6 Motivation and Research Objective

1.6.1 Motivation

The motivation for the present research on HPM source MILO is led by its potential application, particularly in defence. MILO has emerged as one of the most promising HPM sources in recent years due to its compactness, lightweight, and efficiency, which enable it to be used as a direct energy weapon and placed on mobile platforms. Significant effort has been made in the past and present to enhance the overall performance of the MILO device, including theoretical, experimental, and simulation work. MILO design improvements to prevent crucial challenges such as pulse shortening, asymmetric mode generation and mode competition, shot-to-shot repeatability, the necessity of high pulse rate frequency, and long cathode life remain a challenge for device development. These aspects motivated the author to associate, contribute, and enhance the knowledge of the HPM oscillator - MILO device.

Kesari *et al.* reported a periodic circular waveguide having both dielectric and metal loading to widen the bandwidth of a gyro-travelling-wave tube (gyro-TWT), which dielectric loading leads to an increase in one more parameter for regulating the dispersion of metal disc-loaded waveguide in the year of 2005. Hashmi reported a modified A6 magnetron in which the cavities were symmetrically filled with low loss dielectric material to improve the RF spectrum of the device in the year 2010. Maurya *et al.* also reported a simulation study on a partially low-loss dielectric-loaded A6 relativistic magnetron in which the RF output power was increased by 40 % as compared to the without dielectric-loaded A6 magnetron in the year 2012. The author is motivated to use the dielectric filling in the MILO device and also analyze the effect of dielectric on various parameters of MILO like effect on dispersion, effect on interaction impedance, the effect on RF phase velocity, etc.

The concept of dielectric loading has been done by Fan *et al.* and they reported that the peak power conversion efficiency increased from 8.5% to 14% through simulation analysis in 2015. Kumar *et al*. have done the PIC simulation study of DFMILO and obtained the efficiency of the device is 14.8% in 2020. Kumar *et al*. have also done the design and simulation of dielectric filled bi-frequency MILO and reported a peak power conversion efficiency ~13.25% in 2021.

Several studies only provide simulation results when using dielectric filling in MILO as well as other HPM devices. This method has been used first time to analyze the effect of dielectric loading inside the cavity formed between the consecutive disks. The present analysis gives detail information of dispersion relation affected by dielectric loading and its dependency on other design parameters. In this thesis temporal growth rate has also been calculated using the present analysis.

The author additionally took advantage of MILO's partial dielectric filling and conducted an analytical investigation to confirm the simulation's findings. Using Maxwell's circular waveguide equations, the author derived the equations for the electric and magnetic fields. By using these equations, the author is able to determine the electromagnetic equations for every region found in the DFMILO and compare both the findings of simulation and those of analytical analysis. The author discovered the results' high degree of agreement.

1.6.2 Research Objective

The prime objective of the thesis is to analyze the partially dielectric-filled MILO by using the field matching approach. So the author partially fills the dielectric material in the SWS cavity. By doing this, another region has occurred in the MILO structure. For analytical analysis, the author employs the field matching approach to deduce the electric and magnetic

field equations for all regions with the help of circular wave guide Maxwell equitation present in the structure. By applying the boundary conditions between different regions, the author analytically deduced the dispersion relation and interaction impedance and compared the result with the simulated result in the beam absent (cold analysis) and beam present (hot analysis) case. In the electron beam present case, in the structure, one additional region is introduced which is the electron beam region. The linearized Maxwell's fluid equation (i.e., Vlasov-Maxwell's equation) has been applied to analyze the region where the electron beam was present.

The author also designs the tapered dielectric-filled MILO where tapering is provided to the SWS cavity. The sharp tapering is provided to the extractor disc inner radius for impedance matching with a coaxial transmission line (CTL) to extract the power and also uses a tapered cathode for explosive emission. The author analyzes the partially dielectric-filled MILO by using an equivalent circuit approach where the inductance and capacitance of the schematic structure depend on the device parameters (i.e., periodicity of structure, the gap between the cathode and SWS cavities, depth of the cavities, etc.). The author also deduced the dispersion from the simulation and compares it with the analytical result. There is close agreement between the simulated and analytical results. The author also describes the effect of temporal growth, which depends on the imaginary frequency. The author introduces a new concept of the cathode misalignment effect. By the effect of cathode misalignment, degenerate modes are generated in the structure. The author also discussed the effect of different degenerate modes on the structure. The whole structure is analyzed when the electron beam is present, and the beam loading effect is also discussed. The modelled structure is simulated with the help of the electron beam using PIC (Particle in Cell) simulation code 'CST Particle studio'.

1.7 Plan and Scope

Because of its self-magnetic insulation, compactness, and lightweight characteristics, the MILO device is considered one of the most widely used HPM devices. This device is stable across a wide voltage range because it does not change its operating frequency when the input DC voltage is changed. MILO offers one of the most potentials among HPM devices for bi-frequency generation with a single HPM device. MILO development and experimental work in HPM sources is always a difficult task due to the participation of several domains such as electromagnetic theory, charged particle optics, dissipation of sufficient power at the anode, plasma formation, thermal effects at the load side, and so on. As a result, it has been decided to improve MILO's analytical, design, modelling, and experimental activities to better understand these elements. The field matching approach is used for the analytical analysis of partially dielectric-filled coaxial structures. Dielectric filling in the MILO, gives an additional tool to control the dispersion curve, thereby also increasing the RF output power due to increasing the effective capacitance in the SWS structure and giving an improved RF spectrum. As a result, the entire research effort, taking into account the aforementioned aims, is contained in the present thesis, which is divided into five chapters as follows:

The first chapter gives an outline of several HPM systems, their applications, and requirements in various domains. The MILO device is found to be an effective HPM source for producing high-power microwaves after a brief description and comparison of other HPM sources. This chapter provides a brief overview of the MILO device's different sub-assemblies as well as the operating principle. A detailed literature review of the development of the MILO device's theory, design, and development is presented. Finally, the motivation and objective of the current thesis work are also explained here.

The second chapter includes the partially dielectrically filled periodic-disc loaded co-axial structure for Magnetic Insulated Line Oscillator (MILO) has been electromagnetically analyzed using Field Matching Technique in the absence of an electron beam (cold analysis). The slow-wave structure includes a periodic disc-loaded coaxial structure in which the low-loss dielectric material is partially filled between successive discs. In the analysis, the dispersion relation and interaction impedance have been calculated inside the structure. The effect of the material's dielectric constant on the dispersion curve and phase velocity has been investigated. Also, the effect of the different structural parameters on the dispersion curve, and the interaction impedance has been obtained. To validate the performed theoretical analysis, the analytically obtained dispersion results have been compared with previously known dispersion results and then also confirmed by the commercial code "CST Studio Suite

The third chapter includes the electromagnetic (or RF) behaviour of the axially periodic disc-loaded coaxial structure investigated in the presence of an electron beam (hot analysis) with the help of the field matching approach. The linearized Maxwell's fluid equation (i.e., Vlasov-Maxwell's equation) has been used to analyze the region in which the electron beam was present. In the analysis, the dispersion relation and temporal growth rate have been calculated inside the structure. The dispersion relation and temporal growth rate are determined on the assumption that a para potential flow equilibrium is established in the electron beam region.

The fourth chapter contains an S-band tapered MILO with partially dielectric-loaded cavities that are proposed to improve the overall efficiency of the MILO device. The tapered interaction cavities of the MILO are partially filled with low-loss dielectric material. An Equivalent circuit analysis is performed to get the dispersion characteristic of the resonating structure of the proposed MILO. An extensive simulation study is carried out to get the

proposed structure's electromagnetic (EM) and RF behaviour using 3D EM simulation tool (i.e., CST Studio Suite). In this study, for the first time, we have explored the S- band tapered MILO with partial dielectric loading and the effect of cathode misalignment on RF output power.

Finally, chapter five summarizes the work described in this present thesis, and significant conclusions are drawn from the major findings. The study's shortcomings are also explored, as well as the potential for future research.